Boundary conditions for envelope functions at interfaces between dissimilar materials

G. T. Einevoll and L. J. Sham
Department of Physics, University of California San Diego, La Jolla, California 92093-0319
(Received 7 September 1993)

In the effective-mass approximation, the validity of the boundary conditions for an envelope function F across an interface between two different materials is predicated on the similarity of the nearest band-edge Bloch functions. Such approximations break down when the two materials are very dissimilar, e.g., a metal and a semiconductor. By studying one-dimensional model potentials we derive more accurate functional relations between the total wave function and its envelope. From these the usual boundary conditions are restored (continuity of F and F'/m^*) when similar band edges are aligned at abrupt interfaces in semiconductor heterostructures. More importantly, we also derive appropriate boundary conditions for the case when band edges with qualitatively different Bloch functions are aligned. In particular, we find unique boundary conditions for interfaces between regions with and without periodic potentials. These boundary conditions are shown to apply to semiconductor heterostructures described within the nested effective-mass approximation and are arguably reasonable approximations for metal-semiconductor interfaces.

I. INTRODUCTION

The effective-mass approximation[1] (EMA) is a simple and extensively used method for determining electronic states in bulk semiconductors. The EMA is on a solid footing in bulk semiconductors where the theory has been shown to be asymptotically exact in the limit of infinitely weak and slowly varying perturbing potentials. Since the advent of semiconductor heterostructures the approximation has been widely applied to these systems as well, even though the use of the EMA is more difficult to justify in this case.[2] In such heterostructures the effective mass m^* is in general position dependent. Since the momentum operator $\mathbf{p}$ and a position-dependent effective mass do not commute, a question concerning the correct form of the kinetic operator has arisen. This question is directly related to the form of the boundary conditions to impose on the envelope functions at abrupt material interfaces.[3] The question regarding operator ordering, or equivalently boundary conditions, has attracted much attention, not only because of its theoretical interest, but also because of its practical importance. For the case of aligned Γ-point conduction-band edges with spherical effective masses and similar band-edge Bloch functions, a single-band EMA is applicable. A wide range of approaches has been taken to determine the appropriate boundary condition to impose at abrupt interfaces for this simplest effective-mass theory. Even though other choices for boundary conditions have appeared in the literature, the choice

$$F = \text{continuous}\ , \quad \frac{1}{m^*}\frac{dF}{dx} = \text{continuous}\ , \tag{1}$$

is the most soundly based. Even though these boundary conditions were used earlier by Conley *et al.*,[4] they are best known as the BenDaniel-Duke boundary conditions,[5] and we will keep this name here. By studying a two-band model White and Sham were able to derive the BenDaniel-Duke boundary conditions in the context of semiconductor heterostructures.[6] Bastard derived the second condition in (1) by assuming the first one.[7] Galbraith and Duggan[8] found this boundary condition to give a good fit when comparing effective-mass results with photoluminescence excitation spectra from GaAs-$Al_{0.35}Ga_{0.75}As$ quantum wells. Einevoll and coworkers[9–11] obtained the conditions (1) by comparing effective-mass results with exact results on exactly solvable one-dimensional heterostructure models. Furthermore, both Young,[12] who studied the case of slowly varying inhomogeneities, and Burt,[13] who used another envelope-function formalism on abrupt heterointerfaces, obtained the same result. The BenDaniel-Duke boundary conditions are only applicable when nondegenerate band edges with similar band-edge Bloch functions are aligned. For heterostructures where band edges with qualitatively different band-edge Bloch functions are aligned, the situation is less satisfactory. An example is Γ-X mixing in GaAs-AlAs superlattices where multiband EMA descriptions with a phenomenological mixing coefficient have been used.[14]

Another important class of heterostructures are the metal-semiconductor structures.[15] A Schottky barrier is formed at an interface between a metal and a doped semiconductor, and its height and shape determine the electronic transport through the interface. The simplest description of this system involves the single-band EMA for the semiconductor and the free-electron approximation for the metal. In order to calculate the tunneling probability through the Schottky barrier, one might be tempted to match the semiconductor envelope function F_s with the metal wave function F_m at the metal-semiconductor interface, and the question arises as to what boundary conditions to use. The BenDaniel-Duke boundary conditions are expected to apply only when band edges with similar band-edge Bloch functions are aligned. Since this criterion is certainly not fulfilled for

the metal-semiconductor system, it is not to be expected that the BenDaniel-Duke boundary conditions are applicable.

In this article we derive boundary conditions for a wide range of situations using a simple and intuitive approach. We consider one-dimensional heterostructures and derive functional relationships between the total wave function Ψ and the single-band envelope function F. At heterointerfaces the total wave function Ψ and its derivative Ψ' must be continuous, and by using the above-mentioned functional relationships, boundary conditions imposed on F and F' are found. The boundary conditions thus obtained depend on all band-edge energies and band-edge Bloch functions of the constituent semiconductors in the heterostructure, and can in principle be calculated for all one-dimensional potentials. However, it would be more useful to have more general boundary conditions given in terms of experimentally observable quantities such as the effective mass, even if they are valid for a limited range of systems only. In this spirit, we obtain for weak periodic potentials the BenDaniel-Duke boundary conditions (1) when band edges with similar conduction-band edges are aligned, except at the lowest band edge. Furthermore, our procedure yields boundary conditions for strained heterostructures and heterostructures where band edges with qualitatively different band-edge Bloch functions are aligned, which are in agreement with results from exact studies of specific examples.[10,11]

With our approach it is also straightforward to derive boundary conditions for the one-dimensional analogue of the metal-semiconductor interface. This question has, to our knowledge, not been addressed before. As our most striking result, we find that the boundary conditions

$$F_s = F_m \ , \tag{2}$$

$$\frac{1}{2}\frac{1}{m_s^*}F_s' = \frac{1}{m_0}F_m' \ , \tag{3}$$

where m_0 is the free-electron mass, are the right choice with some caveats. The difference from the BenDaniel-Duke boundary conditions lies in the factor $\frac{1}{2}$ on the semiconductor side of Eq. (3).

The new boundary conditions are obtained on the basis of one-dimensional models, some of whose properties do not hold in real three-dimensional systems. However, these boundary conditions may well apply to realistic layered heterostructures, since the conditions are consistent with the particle flux continuity along the growth axis averaged over a unit-cell cross section.[16] In addition to possible applications to effective-mass theory for three-dimensional systems, our results are directly applicable to realistic heterostructures described by the recently introduced *nested* effective-mass approximation (NEMA).[17] In Ref. 17 the NEMA was introduced as a simple way of describing electronic states in superlattices of superlattices, which are structures consisting of periodically alternating superlattices. In this approximation, superlattice sections in semiconductor heterostructures are represented by their position-dependent miniband edges and associated miniband-edge effective masses. It was demonstrated in concrete cases that in many situations of practical interest the NEMA provides accurate results. In the NEMA the wave functions in the plane of the heterointerface are simply plane waves, and the in-plane directions trivially vanish from the description. Thus the one-dimensional results found here apply directly.

In Sec. II general expressions for the functional relationships between the total wave function Ψ and its derivative Ψ', and the envelope function F and its derivative F', are obtained. In Sec. III these relationships are used to derive boundary conditions for the envelope function in semiconductor heterostructures for a wide range of situations. In Sec. IV we derive boundary conditions for metal-semiconductor systems and give examples of their application. A discussion is given in the final Sec. V.

II. THE EFFECTIVE-MASS APPROXIMATION

Our starting point is the well-established effective-mass approximation for bulk semiconductors.[1] Below we will proceed initially in the same way as Altarelli[16] and list the main results in this version of deriving an EMA description for impurity states. For a more complete derivation we refer to Ref. 16. The wave function Ψ of a perturbed state in a bulk semiconductor (for example due to an impurity) satisfies the equation

$$\left[-\frac{\hbar^2}{2m_0}\nabla^2 + V(\mathbf{r}) + U(\mathbf{r})\right]\Psi \equiv [H_0 + U(\mathbf{r})]\Psi = E\Psi \ , \tag{4}$$

where H_0 is the unperturbed crystal Hamiltonian, and $U(\mathbf{r})$ is an additional slowly varying potential. Ψ is expanded in eigenfunctions of H_0, namely,

$$\Psi(\mathbf{r}) = \sum_{n\mathbf{k}} \Phi_n(\mathbf{k})\psi_{n\mathbf{k}}(\mathbf{r}) \ , \tag{5}$$

where

$$H_0\psi_{n\mathbf{k}} = E_{n\mathbf{k}}\psi_{n\mathbf{k}} \ . \tag{6}$$

Substituting (5) in Eq. (4) gives for the coefficient functions $\Phi_n(\mathbf{k})$

$$(E_{n\mathbf{k}} - E)\Phi_n(\mathbf{k}) + \sum_{n'\mathbf{k}'}\langle\psi_{n\mathbf{k}}|U(r)|\psi_{n'\mathbf{k}'}\rangle\Phi_{n'}(\mathbf{k}') = 0 \ . \tag{7}$$

If the energy E of the perturbed state is close to the nth band edge and far from all other band edges, and $U(\mathbf{r})$ is shallow and changes little over one lattice spacing, the EMA can be applied. In this approximation Eq. (7) simplifies to

$$(E_{n\mathbf{k}} - E)\Phi_n(\mathbf{k}) + \sum_{\mathbf{k}'}\hat{U}(\mathbf{k}-\mathbf{k}')\Phi_n(\mathbf{k}') = 0 \ , \tag{8}$$

where $\hat{U}$ is the Fourier transform of $U(\mathbf{r})$. The EMA equation in real space is essentially the Fourier transform of (8), and for a perturbed state close to an isotropic, nondegenerate band edge at $\mathbf{k}=\mathbf{0}$ one finds

$$\left[-\frac{\hbar^2}{2m_n^*}\nabla^2 + U(\mathbf{r})\right] F_n(\mathbf{r}) = (E - E_{n0})F_n(\mathbf{r}) , \quad (9)$$

where the envelope function $F_n(\mathbf{r})$ is the Fourier transform of $\Phi_n(\mathbf{k})$, m_n^* is the effective mass, and E_{n0} is the energy at the nth band edge. In order to relate the envelope function F_n to the total wave function Ψ, the periodic part of the Bloch function $\psi_{n\mathbf{k}}$ is expanded around the band minimum at $\mathbf{k}=\mathbf{0}$ using standard $\mathbf{k}\cdot\mathbf{p}$ theory. This gives

$$\Psi(\mathbf{r}) = F_n(\mathbf{r})\psi_{n0}(\mathbf{r}) + \sum_{m\neq n} \frac{-i\hbar\nabla F_n(\mathbf{r})\cdot\mathbf{p}_{mn}}{m_0(E_{n0}-E_{m0})}\psi_{m0}(\mathbf{r}) + O(\nabla^2 F_n) , \quad (10)$$

where

$$\mathbf{p}_{mn} = \frac{\int \psi_{m0}^*(\mathbf{r})(-i\hbar\nabla)\psi_{n0}(\mathbf{r})d\mathbf{r}}{\int \psi_{m0}^*(\mathbf{r})\psi_{m0}(\mathbf{r})d\mathbf{r}} . \quad (11)$$

In the derivation of the EMA equation (9) the interband matrix elements of the type $\langle\psi_{n\mathbf{k}}|U(r)|\psi_{n'\mathbf{k}'}\rangle$ have been omitted. These matrix elements yield corrections to the wave function of the order $|\hbar\mathbf{p}_{mn}\nabla U/m_0(E_n - E_m)^2|$, smaller than the terms in Eq. (10). Thus, if the external potential is sufficiently slowly varying *at* the interface, these corrections can be safely neglected when deriving boundary conditions for F_n.

From the $\mathbf{k}\cdot\mathbf{p}$ perturbation theory one also obtains a formula for the isotropic effective mass, namely,

$$\frac{1}{m_n^*} = \frac{1}{m_0} + \frac{2}{m_0^2}\sum_{m\neq n}\frac{|p_{nm}^x|^2}{E_{n0}-E_{m0}} . \quad (12)$$

In Eqs. (10) and (12) the sum over m goes over all band edges with an extremal point at $\mathbf{k}=\mathbf{0}$. Considering only the lowest-order term in (10), F_n can be viewed as a slowly varying modulation of the rapidly varying band-edge Bloch function. However, the term involving the gradient of F_n must be kept in order to derive boundary conditions to impose on F_n at heterointerfaces. It is this essential inclusion of the second term in the matching of wave functions at interfaces which makes it possible to relax the usual explicit or implicit assumption of having identical band-edge Bloch wave functions on two sides of the interface (although with different band-edge energies).

We now restrict our considerations to one-dimensional crystals with a symmetric potential around the center of the Wigner-Seitz cell. The one-dimensional versions of Ψ and its gradient Ψ' are, from Eq. (10),

$$\Psi(x) = F_n(x)\psi_{n0}(x) + F_n'(x)\sum_{m\neq n}\frac{-i\hbar p_{mn}}{m_0(E_{n0}-E_{m0})}\psi_{m0}(x) + O[F_n''(x)] , \quad (13)$$

$$\Psi'(x) = F_n(x)\psi_{n0}'(x) + F_n'(x)\psi_{n0}(x) + F_n'(x)\sum_{m\neq n}\frac{-i\hbar p_{mn}}{m_0(E_{n0}-E_{m0})}\psi_{m0}'(x) + O[F_n''(x)]. \quad (14)$$

For the one-dimensional crystals all band extrema are either at the zone center $k=0$ or at the zone edge $k=\pi/a$ (where a is the lattice constant). The derivation of the EMA equation (9) and the functional relation between Ψ and F_n are straightforward to generalize to the case where the band extremum is at the zone edge. Equations (10)–(14) are still valid if $\psi_{n0}(x)$ is replaced with the Bloch function at the zone edge $\psi_{n\frac{\pi}{a}}(x)$, and the sum over band edges is set to include only band edges at $k=\pi/a$. The band-edge Bloch function is biperiodic, i.e., $\psi_{n\frac{\pi}{a}}(x) = -\psi_{n\frac{\pi}{a}}(x+a) = \psi_{n\frac{\pi}{a}}(x+2a)$. For notational simplicity we will in the following denote the band-edge Bloch functions $\psi_n(x)$ both for $k=0$ and $k=\pi/a$ so that Eqs. (10)–(14) apply for both cases. Likewise we will omit the subscript 0 from the symbols for band-edge energies and the subscript n from the envelope function F_n.

In Fig. 1 the possible symmetries for the Bloch function at band extrema with symmetric atomic potentials are illustrated. For band extrema at the zone center the band-edge Bloch function ψ_n is either (i) of even parity about the center of the Wigner-Seitz cell with zero derivative at the Wigner-Seitz cell boundary, or (ii) of odd parity about the cell center and zero at the boundary. For band extrema at the zone edge the band-edge Bloch function also has two distinct possibilities, namely, (iii) of odd parity about the cell center and zero derivative at the boundary or (iv) of even parity about the cell center and zero at the boundary. For later use we will designate band edges in categories (i) and (iii) as class I, while band edges in categories (ii) and (iv) are called class II.

In order to derive boundary conditions for the envelope function, the total wave function Ψ and its derivative Ψ' must be evaluated at the boundary of the Wigner-Seitz cell. We first focus on a band edge n of class I where the derivative of the Bloch function vanishes at a cell boundary set to be at $x=0$, i.e., $\psi_n'(0)=0$. In this case the contribution from the sum in Eq. (13) vanishes since $p_{mn}\psi_m(0)=0$ for all m. This follows from the fact that $p_{mn}\neq 0$ only when $\psi_n(x)$ and $\psi_m(x)$ have differ-

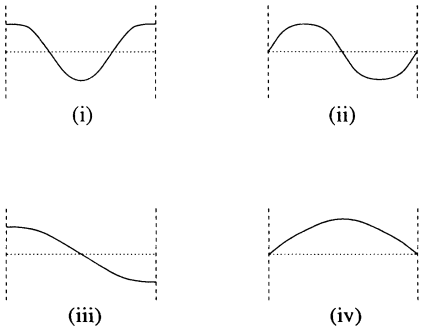

FIG. 1. Sketches of the four symmetry categories of band-edge Bloch functions ψ_n for one-dimensional periodic potentials. Categories (i) and (ii) occur for band edges at $k=0$, while categories (iii) and (iv) occur for $k=\pi/a$. Band edges in category (i) or (iii) are labeled class I in this article, while band edges in category (ii) or (iv) are labeled class II.

ent parity. When $\psi_m(x)$ has different parity from $\psi_n(x)$, however, $\psi_m(0)$ is always zero. Thus the leading terms in Eqs. (13) and (14), evaluated at the Wigner-Seitz cell boundary, simplify to

$$\Psi(0) = F(0)\psi_n(0) , \tag{15}$$

$$\Psi'(0) = F'(0)\psi_n(0) + F'(0)\sum_{m\neq n}\frac{-i\hbar p_{mn}}{m_0(E_n-E_m)}\psi'_m(0)$$
$$\equiv a_n F'(0)\psi_n(0) , \tag{16}$$

where

$$a_n \equiv 1+\sum_{m\neq n}\frac{-i\hbar p_{mn}}{m_0(E_n-E_m)}\frac{\psi'_m(0)}{\psi_n(0)} . \tag{17}$$

For band edges of class II, the Bloch functions themselves vanish at the cell boundary, i.e., $\psi_n(0)=0$. In this case the sum in Eq. (14) vanishes since $p_{mn}\psi'_m(0)$ is zero for all m. This is because $p_{mn}\neq 0$ only when $\psi'_m(0)=0$. Equations (13) and (14) evaluated at the cell boundary thus reduce to

$$\Psi(0) = F'(0)\sum_{m\neq n}\frac{-i\hbar p_{mn}}{m_0(E_n-E_m)}\psi_m(0) \equiv b_n F'(0)\psi'_n(0) , \tag{18}$$

$$\Psi'(0) = F(0)\psi'_n(0) , \tag{19}$$

where

$$b_n \equiv \sum_{m\neq n}\frac{-i\hbar p_{mn}}{m_0(E_n-E_m)}\frac{\psi_m(0)}{\psi'_n(0)} . \tag{20}$$

An important observation from Eqs. (15)–(20) is that the leading terms in the functional relationships between cell boundary values of Ψ and Ψ' and the envelope function divide into two distinct classes. For class-I band edges $\Psi(0)$ is proportional to $F(0)$, while $\Psi'(0)$ is proportional to $F'(0)$. For class-II band edges $\Psi(0)$ is proportional to $F'(0)$, while $\Psi'(0)$ is proportional to $F(0)$. If Ψ and Ψ' of two semiconductors with band edges belonging to the same class are matched at an interface taken to be at the Wigner-Seitz cell boundary, the boundary conditions for the envelope function will couple F (F') on one side of the interface with F (F') on the other. However, if Ψ and Ψ' of two semiconductors with band edges belonging to different classes are matched at an interface, the boundary conditions for the envelope function will couple F on one side of the interface to F' on the other.

Even in the absence of a perturbing potential $U(\mathbf{r})$ the expressions (15), (16), (18), and (19) are only approximations. The corrections to the relations (15) and (19), where the dominant term is proportional to $F(0)$, are of order F''. Correspondingly, the corrections to the relations (16) and (18), where the dominant term is proportional to $F'(0)$, are of order F'''. Thus the corrections are in both cases typically of order k^2, where k is a characteristic wave number of the envelope function for the eigenstate in question. For states energetically close to the nth band edge, k is small and the formulas (15), (16), (18), and (19) are valid.

The coefficients a_n and b_n in (17) and (20) can in principle be calculated for all one-dimensional (symmetric) potentials. However, it would be more useful to have more general, though approximate, expressions for a_n and b_n valid for a wide range of potentials. Moreover, it would be even more desirable to have expressions involving only quantities which can be measured experimentally, such as for example the effective mass m^*. We will address this question in the next section.

III. SEMICONDUCTOR HETEROSTRUCTURES

We now consider weak one-dimensional periodic potentials where the band structure essentially is free-electron-like except at $q_j = \pm j\pi/a$, $j = 1,2,3,\ldots$, (in the extended zone picture) where gaps open up. For weak potentials the size of the gap is $2|V(2q_j)|$, where $|V(2q_j)|$ is the Fourier transform of the perturbing periodic potential. In the sum over band edges in the expressions for m_n^*, a_n, and b_n [(12),(17),(20)] the energy differences between the band edges appear in the denominator. For weak potentials where the gaps are small, the contribution from the adjacent band edge l will dominate. Thus in the weak-potential regime the expression for the effective mass at band edge n is approximately given by

$$\frac{1}{m_n^*} = \frac{1}{m_0}+\frac{2}{m_0^2}\sum_{m\neq n}\frac{p_{nm}p_{mn}}{E_n-E_m} \simeq \frac{2}{m_0^2}\frac{p_{nl}^0 p_{ln}^0}{E_n-E_l} . \tag{21}$$

Here p_{nl}^0 denotes the matrix element (11) between the zeroth-order Bloch functions. The final expression in (21) is of order V^{-1}, and the corrections are of order V^0. This is similar in spirit to the two-band model of White and Sham[6] (see also Bastard[7] and Eppenga *et al.*[18]).

First we focus on conduction- or valence-band edges of class I. In this case we have from Eqs. (15) and (16) $\Psi(0) = F(0)\psi_n(0)$ and $\Psi'(0) = a_n F'(0)\psi_n(0)$. For weak potentials a_n can be approximated as

$$a_n = 1+\sum_{m\neq n}\frac{-i\hbar p_{mn}}{m_0(E_n-E_m)}\frac{\psi'_m(0)}{\psi_n(0)}$$
$$\simeq \frac{-i\hbar p_{ln}^0}{m_0(E_n-E_l)}\frac{\psi_l^{0\prime}(0)}{\psi_n^0(0)} \simeq \frac{m_0}{2m_n^*}\frac{-i\hbar\psi_l^{0\prime}(0)}{p_{nl}^0\psi_n^0(0)} . \tag{22}$$

Here we have used Eq. (21) and introduced the notation ψ_n^0 for the unperturbed Bloch function at band edge n. With a Wigner-Seitz cell located between 0 and a, the appropriate Bloch function is given by

$$\psi_n^0(x) = \sqrt{\frac{2}{a}}\cos(q_j x) , \tag{23}$$

$$q_j = \frac{j\pi}{a},\ j = 1,2,3,\ldots , \tag{24}$$

where even and odd values of j correspond to band edges at $k=0$ and $k=\pi/a$, respectively. The Bloch function at the adjacent band edge is

$$\psi_l^0(x) = \sqrt{\frac{2}{a}}\sin(q_j x) . \tag{25}$$

Then simple algebra gives

$$\frac{-i\hbar\psi_l^{0\prime}(0)}{p_{nl}^0\psi_n^0(0)} = 1 , \tag{26}$$

so that to dominant order in V one ends up with

$$\Psi(0) = F(0)\psi_n(0) , \tag{27}$$

$$\Psi'(0) = \frac{m_0}{2m_n^*}F'(0)\psi_n(0) . \tag{28}$$

Next we discuss band edges of class II. From Eqs. (18) and (19) we have $\Psi(0) = b_n F'(0)\psi_n'(0)$ and $\Psi'(0) = F(0)\psi_n'(0)$. Again, for weak potentials b_n is approximately given as

$$b_n = \sum_{m\neq n}\frac{-i\hbar p_{mn}}{m_0(E_n - E_m)}\frac{\psi_m(0)}{\psi_n'(0)}$$
$$\simeq \frac{-i\hbar p_{ln}^0}{m_0(E_n - E_l)}\frac{\psi_l^0(0)}{\psi_n^{0\prime}(0)} \simeq \frac{m_0}{2m_n^*}\frac{-i\hbar\psi_l^0(0)}{p_{nl}^0\psi_n^{0\prime}(0)} . \tag{29}$$

The band-edge Bloch functions are now given by (25) while the Bloch functions at the adjacent band edges are given by (23). Then one finds

$$\frac{-i\hbar\psi_l^{0\prime}(0)}{p_{nl}^0\psi_n^0(0)} = -\frac{1}{q_j^2} , \tag{30}$$

so that to dominant order in V one now ends up with

$$\Psi(0) = -\frac{1}{q_j^2}\frac{m_0}{2m_n^*}F'(0)\psi_n'(0) , \tag{31}$$

$$\Psi'(0) = F(0)\psi_n'(0) . \tag{32}$$

Note that the results (27), (28), (31), and (32) are independent of the choice of sign and normalization factors for the band-edge Bloch functions. Also one gets the same results for the Wigner-Seitz cell boundary located at $x = a$.

The effective mass m_n^* in Eqs. (28) and (31) is the *electron* effective mass which can be either positive or negative. While the expressions above are valid also for valence-band edges where m_n^* is negative, it is more customary to use the hole mass, defined as $-m_n^*$, in these cases.

We can now derive boundary conditions to impose on the envelope function at a material interface for systems in the weak-potential regime. The heterostructure is assumed to be built up of Wigner-Seitz cells joined together so that the material interface is located at a boundary between two different Wigner-Seitz cells. The boundary conditions for F and F' follow from the required continuity of Ψ and Ψ' at this interface.

First we consider an interface where the band edges (labeled A and B) which are aligned are both of class I. Then from the continuity of Ψ and Ψ' in (27) and (28) one obtains the boundary conditions

$$F_A(0)\psi_A(0) = F_B(0)\psi_B(0) , \tag{33}$$

$$\frac{1}{m_A^*}F_A'(0)\psi_A(0) = \frac{1}{m_B^*}F_B'(0)\psi_B(0) , \tag{34}$$

where we have canceled the common factor $m_0/2$ in (34) and omitted the subscript n for notational simplicity. Only the ratio F'/F is of physical importance. We will therefore for compactness describe boundary conditions only by this ratio in the following. For the boundary conditions above one obtains

$$\frac{1}{m_A^*}\frac{F_A'(0)}{F_A(0)} = \frac{1}{m_B^*}\frac{F_B'(0)}{F_B(0)} . \tag{35}$$

These boundary conditions are recognized as the BenDaniel-Duke boundary conditions discussed in the Introduction.

Next we consider a heterointerface where two band edges of class II are aligned. From (31) and (32) one finds

$$\frac{1}{q_A^2}\frac{1}{m_A^*}\frac{F_A'(0)}{F_A(0)} = \frac{1}{q_B^2}\frac{1}{m_B^*}\frac{F_B'(0)}{F_B(0)} . \tag{36}$$

Here $q_{A,B} = j\pi/a_{A,B}$ $(j = 1, 2, 3, \ldots)$ is the wave vector at the point in the Brillouin zone where the band gap in question opens up. If the two crystals which are joined together at the heterointerface have the same lattice constant, and the aligned band edges correspond to the same gap, q_A equals q_B. Then the boundary condition (36) reduces to the BenDaniel-Duke condition (35). If the lattice constants are different while the aligned band edges correspond to the same gap, i.e., same j, the boundary condition turns into

$$\frac{a_A^2}{m_A^*}\frac{F_A'(0)}{F_A(0)} = \frac{a_B^2}{m_B^*}\frac{F_B'(0)}{F_B(0)} . \tag{37}$$

Thus for strained heterostructures where the longitudinal lattice constant varies with position, the lattice constant also enters into the boundary condition.

It is gratifying that our procedure always yields the BenDaniel-Duke boundary conditions when band edges of the same type are aligned, and the lattice constant is the same on both sides of the heterointerface. It should be noted, however, that the BenDaniel-Duke boundary conditions are apparently only generally applicable when the periodic potential in the semiconductor is weak, i.e., when the dominant term in the $\mathbf{k}\cdot\mathbf{p}$ perturbation sum (for the effective mass and wave function) comes from the two bands forming the narrow band gap. In semiconductors with small conduction-band effective masses such as GaAs and InAs, this criterion is well fulfilled and the BenDaniel-Duke boundary condition should be applicable. The requirement of including the lattice constant in the boundary conditions for strained heterostructures is not new. In recent studies[10,11] boundary conditions were obtained by considering simple Kronig-Penney δ-function periodic potentials in one dimension. For heterostructures made up of Kronig-Penney materials exact closed-form expressions for the eigenstate energies can be obtained. By comparing exact results with approximate EMA results for states close to the conduction-band edge, it was found that the EMA is valid if, and only if, the boundary conditions (35) and (36) are used for class-I and class-II band edges, respectively. In fact it was found that these boundary conditions ensure asymptotic agreement between EMA results and exact results in the limit when the eigenstate energies approach the conduction-band edges, for arbitrary values of the strength of the δ-well potential. However, the observed validity of (35) and (36)

in the strong-potential limit at conduction-band edges in Kronig-Penney potentials is not generalizable to all one-dimensional potentials. In the Appendix we have calculated the coefficients a_n (17) for a class-I conduction-band edge and b_n (20) for a class-II conduction-band edge in Kronig-Penney δ-well crystals to the next lowest order in the δ-well strength. The corrections to (28) and (31) are found to be identically zero, in agreement with the observation in Refs. 10 and 11.

An important point is that none of the boundary conditions above apply to the lowest band edge (labeled 0), i.e., to the bottom of the only "band" present in the free-electron case. This can be shown by the following simple argument: At the lowest band edge the zeroth-order Bloch function is simply a constant, which means (i) the band edge is of class I, and (ii) p^0_{0m} is zero for all m. The perturbing weak potential couples ψ^0_m from other band edges into ψ_0, and the leading term in $p_{0m} \propto \langle\psi_0|d/dx|\psi_m\rangle$ is found to be of order V. For the lowest band edge all the energy differences in the denominator of the sums in (12) and (17) are of order V^0. Thus from (12) one sees that the inverse effective mass will be of the form

$$\frac{m_0}{m_0^*} = 1 + c_1 V^2 + O(V^3) \,. \tag{38}$$

Since the derivative of the band-edge Bloch function is zero, we consider Eqs. (15)–(17) to find Ψ and Ψ' at the Wigner-Seitz cell boundary. The dominant term in the sum in the expression for a_0 (17) is of order V. Thus for small V the ratio between $\Psi'(0)$ and $\Psi(0)$ has the form

$$\frac{\Psi'(0)}{\Psi(0)} = \left(1 + c_2 V + O(V^2)\right) \frac{F'(0)}{F(0)} \,. \tag{39}$$

Since in (38) the correction to the free-electron mass is seen to be of order V^2, it is obvious that (39) is only compatible with the BenDaniel-Duke boundary conditions to $O(V^0)$ (where $m_0^* = m_0$). The results above suggest that the best approximation is to use the free-electron mass combined with the "normal" boundary conditions

$$\frac{F'_A(0)}{F_A(0)} = \frac{F'_B(0)}{F_B(0)} \tag{40}$$

for heterostructure states energetically close to these lowest band edges.

The EMA has predominantly been used for semiconductors where the aligned band edges have extremal points at the same point in the Brillouin zone. For heterostructures where widely separated extremal points contribute to the wave function, the conventional EMA is unable to account for the mixing. Since the conduction bands of GaAs and AlAs have global minima at the Γ point ($\mathbf{k} = \mathbf{0}$) and X point (close to the zone edge), respectively, effects of Γ-X mixing has been sought in GaAs-AlAs heterostructures in the tight-binding approximation.[19] Attempts have been made to extend the EMA to describe Γ-X mixing, but the extensions have not always been based on microscopic considerations. Such extensions have been made at the expense of adding new parameters to the effective-mass description.[14,20]

The one-dimensional analogue to Γ-X mixing is mixing between band edges with extremal points at $k = 0$ and $k = \pi/a$. Boundary conditions for the case when band edges at different extremal points are aligned can be found from the expressions (27), (28), (31), and (32) valid for weak periodic potentials. Let us consider for instance a heterostructure where a conduction-band edge at $q_A = j_A\pi/a_A$ with even j_A is aligned with a conduction-band edge at $q_B = j_B\pi/a_B$ with odd j_B. Furthermore, let us assume that the atomic potentials are such that the Fourier transforms $V(2q_A)$ and $V(2q_B)$ are negative. Then band edge A will be of class II with the minimum located at $k = 0$, while band edge B will be of class I with the minimum at $k = \pi/a_B$. Continuity of Ψ and Ψ' at the interface then gives the boundary conditions

$$-\frac{1}{q_A^2}\frac{m_0}{2m_A^*}\frac{F'_A(0)}{F_A(0)} = \frac{2m_B^*}{m_0}\frac{F_B(0)}{F'_B(0)} \,. \tag{41}$$

It has been shown that these "inverted" boundary conditions assure agreement between EMA and exact results for a one-dimensional "Γ-X" Kronig-Penney δ-well superlattice for states energetically close to both conduction-band edges.[21] It is interesting that a superlattice described by single-band EMA, where the wave function is alternately Γ-like ($k=0$) and X-like ($k=\pi/a$) in consecutive superlattice layers, gives an accurate description, and that a multiband description is superfluous in this case. However, a single-band EMA is not appropriate if the Γ and X valleys in both materials are close in energy.

In one-dimensional systems an interface matrix, which relates F_A and F'_A on one side of an interface with F_B and F'_B on the other, has been shown to be either purely diagonal or purely off-diagonal.[20] The boundary conditions (35) and (36) correspond to the diagonal case, while the "inverted" boundary condition (41) corresponds to the off-diagonal case.

IV. METAL-SEMICONDUCTOR INTERFACES

With the results from the previous section, it is straightforward to derive boundary conditions for the one-dimensional analogue to a metal-semiconductor interface. For the metal we use the free-electron approximation, while the semiconductor is modeled with a weak periodic potential as in the previous section. Since the periodic potential is absent in the free-electron approximation, there are no underlying periodic Bloch functions in the metal, and the (total) metal wave function is simply denoted F_m. This wave function must be matched with the total semiconductor wave function at the interface.

With the use of Eqs. (27) and (28) one obtains for semiconductor band edges of class I

$$\frac{1}{2}\frac{1}{m_n^*}\frac{F'_s(0)}{F_s(0)} = \frac{1}{m_0}\frac{F'_m(0)}{F_m(0)} \,. \tag{42}$$

The new and striking factor 1/2 on the semiconductor side of the equation distinguishes this boundary condi-

tion from the BenDaniel-Duke condition. The necessity and importance of this factor will be demonstrated in concrete applications later in this section.

For semiconductor band edges of class II one correspondingly obtains from Eqs. (31) and (32)

$$-\frac{1}{2}\frac{1}{q_j^2}\frac{1}{m_n^*}\frac{F_s'(0)}{F_s(0)} = \frac{1}{m_0}\frac{F_m(0)}{F_m'(0)} \ . \tag{43}$$

Except for the factor 1/2 this boundary condition has some similarity to the "inverted" boundary condition obtained for the Γ-X mixing case in the previous section.

As an application of these boundary conditions we consider electronic transmission through a barrier superlattice (Fig. 2). The transmission probability through any one-dimensional potential profile is easily calculated numerically using the transfer-matrix technique. For the barrier superlattice the transmission probability can also be calculated using the nested effective-mass approximation.[17] In the NEMA the periodic superlattice potential is replaced with its miniband edges and miniband-edge effective masses (see Fig. 2). For energies close to miniband edges, where the NEMA is expected to be valid, the transmission coefficient can be evaluated analytically. However, the question arises as to what boundary conditions to use on the edges of the barrier-superlattice region. These edges are interfaces between regions with and without periodic potentials and thus correspond to the one-dimensional metal-semiconductor interfaces discussed above.

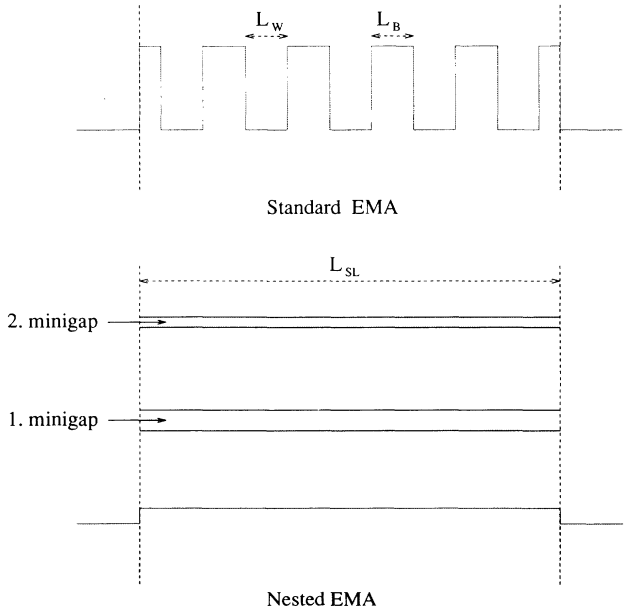

FIG. 2. Qualitative sketches illustrating the difference between the standard EMA picture and the NEMA picture for the case of electrons tunneling through a barrier superlattice. The upper portion shows the standard EMA picture with a position-dependent conduction-band edge representing the superlattice. The lower portion shows the simpler NEMA picture where the barrier superlattice is represented by its miniband edges (and corresponding superlattice effective masses). Only the first and second miniband gaps are shown. The edges of the barrier-superlattice region, which correspond to metal-semiconductor interfaces in the NEMA picture, are indicated (dashed lines).

To test the boundary conditions we calculate the transmission probability analytically in the NEMA and compare with exact results obtained numerically for the periodic square-well potential (within the standard EMA). We focus on miniband edges *above* miniband gaps and thus have positive superlattice effective masses. In the numerical example below we focus on energies close to the class-I miniband edge above the first miniband gap. With the class-I metal-semiconductor boundary condition (42) the NEMA transmission probability is found to be

$$T = \left(\cos^2(qL_{\rm SL}) + m_0^2 m_{\rm SL}^{*2} \frac{q^2/4m_{\rm SL}^{*2} + k^2/m_0^2}{k^2 q^2} \sin^2(qL_{\rm SL}) \right)^{-1} , \tag{44}$$

where

$$q = \sqrt{\frac{2m_{\rm SL}^*}{\hbar^2}(E - E_{\rm SL})} \ , \quad k = \sqrt{\frac{2m_0}{\hbar^2}E} \ . \tag{45}$$

Here $L_{\rm SL}$ is the width of the barrier superlattice region, $E_{\rm SL}$ refers to the energy of the miniband edge, and $m_{\rm SL}^*$ is the superlattice effective mass. Correspondingly, the transmission probability using BenDaniel-Duke boundary conditions is

$$T = \left(\cos^2(qL_{\rm SL}) + \frac{1}{4} m_0^2 m_{\rm SL}^{*2} \frac{q^2/m_{\rm SL}^{*2} + k^2/m_0^2}{k^2 q^2} \sin^2(qL_{\rm SL}) \right)^{-1} . \tag{46}$$

Results from a comparison between exact numerical results and the approximate NEMA formulas using class-I boundary conditions (44) and BenDaniel-Duke boundary conditions (46), respectively, are shown in Fig. 3. In this example the barrier potential is small compared to the miniband widths, and we have used the analytical formula from Ref. 22, valid for weak superlattice potentials, for the superlattice effective mass $m_{\rm SL}^*$. The miniband-edge energy $E_{\rm SL}$ has been obtained numerically. In our example the superlattice region consists of 200 barriers, and the transmission probability for energies corresponding to miniband gaps is negligible. From Fig. 3 it is evident that, while the use of the BenDaniel-Duke conditions gives substantial errors, the use of our new class-I band-edge metal-semiconductor boundary condition gives results in perfect agreement with the exact curve close to the miniband edge. To demonstrate this further it is useful to expand the expression for the transmission probability above the miniband edge. We then find

$$T(E) \simeq \left(\cos^2(qL_{\rm SL}) + \frac{m_{\rm SL}^*}{m_0} \frac{E_{\rm SL}}{E - E_{\rm SL}} \sin^2(qL_{\rm SL}) \right)^{-1} \tag{47}$$

for the class-I band-edge boundary condition and

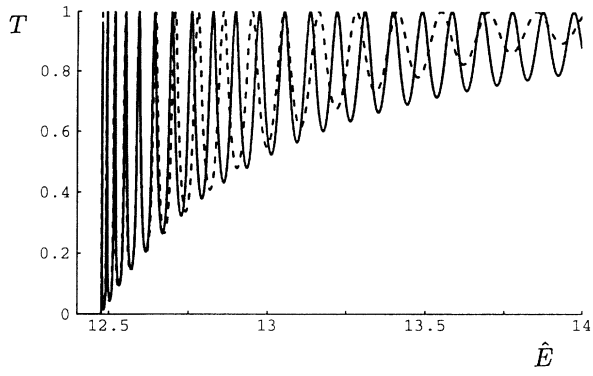

(a)

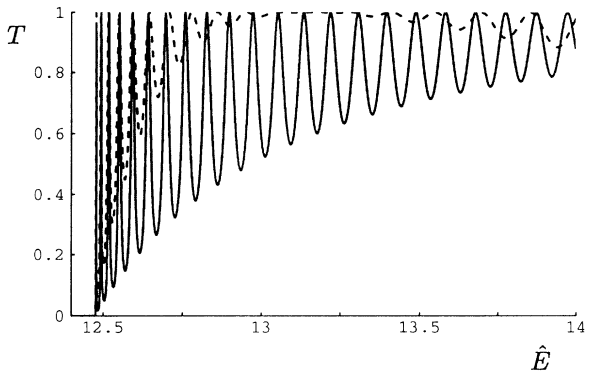

(b)

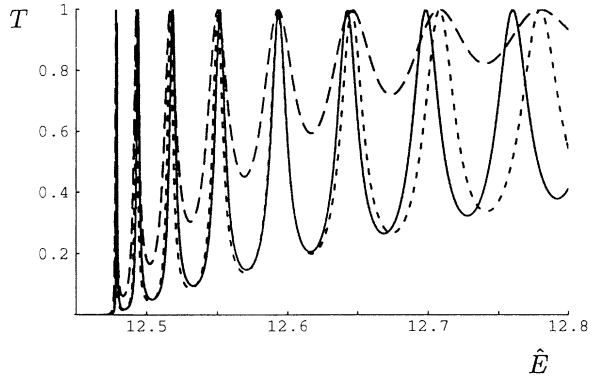

(c)

FIG. 3. Electron transmission probability through a barrier superlattice consisting of 200 barriers. The well (L_W) and barrier (L_B) widths are equal. The dimensionless energy $\hat{E}$ is given by $\hat{E} = E/[\hbar^2/2m_0(L_W + L_B)^2]$. The barrier height is $3.2\hbar^2/2m_0(L_W + L_B)^2$. Results for the energy region above the first miniband gap are shown. In (a) a comparison between exact results (solid) and NEMA results (dotted) using our class-I band-edge boundary conditions (44) is shown. Correspondingly, in (b) a comparison between exact results (solid) and NEMA results (dotted) using BenDaniel-Duke boundary conditions (46) is given. In (c) the energy region directly above the miniband gap is magnified to demonstrate clearly that while NEMA results with class-I band-edge boundary conditions (dotted) agree perfectly with exact results (solid) in this region, the NEMA results using BenDaniel-Duke boundary conditions (dashed) deviate significantly.

$$T(E) \simeq \left(\cos^2(qL_{\rm SL}) + \frac{1}{4}\frac{m^*_{\rm SL}}{m_0}\frac{E_{\rm SL}}{E - E_{\rm SL}}\sin^2(qL_{\rm SL})\right)^{-1} \tag{48}$$

for the BenDaniel-Duke condition. The factor 1/4 in (48) manifests itself in too steep a rise by a factor 4 of a curve drawn through the local minima [where $\cos(qL_{\rm SL}) = 0$] in the transmission probability directly above the miniband edge in Fig. 3(c). For completeness we also give the corresponding transmission probability assuming "normal" boundary conditions, i.e., continuity of the envelope function and its derivative, which is found to be

$$T(E) \simeq \left(\cos^2(qL_{\rm SL}) + \frac{1}{4}\frac{m_0}{m^*_{\rm SL}}\frac{E_{\rm SL}}{E - E_{\rm SL}}\sin^2(qL_{\rm SL})\right)^{-1} . \tag{49}$$

Since $m^*_{\rm SL}/m_0 \sim 0.05$ in our example, this formula gives far too slow a rise of the curve drawn through local minima of the transmission probability above the miniband edge.

In the numerical example in Fig. 3 both the first and the last barrier in the superlattice section have half the width of the other barriers. However, we have numerically found the transmission probability to be insensitive to the widths of the first and last barrier. Thus the NEMA treatment with the new boundary conditions seems robust against changes in details in the potential configuration at the entrance and exit interfaces of the superlattice section. It should be emphasized that the validity of our boundary conditions (42) and (43) (and, correspondingly, the error encountered in using previous boundary conditions) has been verified by comparisons with exact results for different miniband edges for a wide range of system parameters.

An interesting point is that if one applies the class-II band-edge boundary condition (43) one obtains the same approximate formula for the transmission probability above the miniband edge as with the class-I band-edge condition (47). This can be qualitatively understood if $F_m \sim \exp(\pm iq_j x)$ where q_j is the wave vector at the band edge. Then it follows that $(F'_m/F_m)^2 \simeq -q_j^2$, and the class-I (42) and class-II (43) boundary conditions are seen to be effectively identical.

In Ref. 10 exactly solvable one-dimensional models of superlattices and quantum wells were studied to determine boundary conditions in semiconductor heterostructures. It was, for example, found that for unstrained heterostructures built up of Kronig-Penney δ-well potentials the BenDaniel-Duke boundary conditions ensured agreement between exact and effective-mass results when conduction-band edges of the same type were aligned. Similarly, this approach can be used as a check of the validity of our boundary conditions. Let us consider a heterostructure with two thick slabs of Kronig-Penney δ-well materials sandwiching a thin slab with no periodic potential. This structure, tailored to test our metal-semiconductor boundary conditions, is just a special case of the quantum wells considered in Ref. 10 with the strength of the δ wells in the middle section set to zero. For certain energies corresponding to gaps in the

Kronig-Penney barriers there will be states localized in the vicinity of the well region. Using the analytic result in Ref. 10 one can readily obtain exact transcendental equations for the energies of these localized states. When comparing with the corresponding effective-mass expressions, one finds that, when the energy of the localized state approaches the conduction-band edge of the barriers, asymptotic agreement between exact and effective-mass results is obtained if, and only if, the boundary conditions (42) and (43) are used for class-I and class-II band edges, respectively. If, on the other hand, the BenDaniel-Duke boundary conditions are used, no such asymptotic agreement is found and effective-mass theory gives erroneous results.

V. DISCUSSION

In this article we have derived boundary conditions for envelope functions at abrupt interfaces for a wide range of situations using a simple and intuitive scheme. The BenDaniel-Duke boundary conditions are found to be applicable for unstrained semiconductor heterostructures when qualitatively similar band edges are aligned and the periodic potentials are weak. However, when qualitatively different band edges are aligned or when the heterostructure is strained, other boundary conditions should be used. Most importantly, we have also derived boundary conditions to impose at metal-semiconductor interfaces.

In deriving the relatively simple boundary conditions in Secs. III and IV we assumed weak periodic potentials in the semiconductor. In this case it follows that in the $\mathbf{k}\cdot\mathbf{p}$ perturbation sum over the bands (for the effective mass and the wave function) the dominant term comes from the two bands forming the narrow band gap, which holds for real semiconductors with small conduction-band effective masses such as GaAs and InAs. An indirect verification of this is the apparent applicability of the BenDaniel-Duke boundary condition, found in the weak-potential limit in Sec. III, to conduction-band states in heterostructures consisting of semiconductors with qualitatively similar band-edge Bloch functions (e.g., GaAs-$Al_xGa_{1-x}As$ with $x<0.4$). The assumption of weak periodic potentials translates to assuming the energy gap to be substantially smaller than the bandwidths. In superlattices the ratio between miniband gaps and miniband widths can be made arbitrarily small by choosing sufficiently low barriers or short superlattice periods. We therefore expect our boundary conditions to be applicable in NEMA calculations in many situations of practical interest.

The fact that the boundary conditions have been derived in one-dimensional systems may seem to pose a more serious limitation to the applicability of our results. However, our results apply directly to semiconductor heterostructures described with the nested effective-mass approximation since the in-plane directions vanish trivially in this description. Regarding the applicability to true three-dimensional systems, it is encouraging that our approach yields the BenDaniel-Duke boundary conditions when similar band edges are aligned, in agreement with previous studies. It would be particularly interesting if our metal-semiconductor boundary conditions could be tested against experiments or more comprehensive theoretical (presumably numerical) work. A natural extension of the work presented here would be to investigate whether our approach could be used directly to derive boundary conditions in two- and three-dimensional systems.

ACKNOWLEDGMENTS

G.T.E. acknowledges the Norwegian Science Council (NFR) for financial support. L.J.S. is supported in part by NSF Grant No. DMR 91-17298.

APPENDIX

In this Appendix we will do a perturbation expansion to calculate the first correction terms to the coefficients a_n (22) and b_n (29) at two conduction-band edges in Kronig-Penney crystals. The perturbing periodic Kronig-Penney potential is taken to be

$$H_{\mathrm{KP}}(x)=-\frac{\hbar^2}{m_0 a}V\sum_{i=-\infty}^{\infty}\delta(x-(i-1/2)a)\,, \tag{A1}$$

so that a δ-function well is positioned in the center of a Wigner-Seitz cell located between 0 and a. V is the dimensionless potential strength. The Kronig-Penney crystals have conduction-band edges at

$$E_{jc}=\frac{\hbar^2 q_j^2}{2m_0}=\frac{\hbar^2 j^2\pi^2}{2m_0 a^2}\,,\ j=1,2,3,\ldots\,, \tag{A2}$$

for all values of V. At these conduction-band edges the effective mass m^*_{jc} is given by[10]

$$\frac{m^*_{jc}}{m_0}=\frac{V}{j^2\pi^2}\ . \tag{A3}$$

Here we will evaluate a_n for a class-I conduction-band edge ($j=1$) and b_n for a class-II conduction-band edge ($j=2$) including terms of order V^{-1} and V^0 in order to look for the first correction terms to the lowest-order expressions. From (17) and (20) we see that p_{mn}, E_n-E_m, $\psi'_m(0)$, and $\psi_m(0)$ must be calculated. For weak potentials the energy difference E_n–E_m between the band edges on each side of a gap is proportional to V while all other energy differences are of order V^0. For the band-edge Bloch functions standard perturbation theory gives

$$\psi_m(x)=\psi^0_m(x)+\sum_{k\neq m}\frac{\langle\psi^0_k|H_{\mathrm{KP}}|\psi^0_m\rangle}{E^0_m-E^0_k}\psi^0_k(x)+\cdots\,, \tag{A4}$$

where ψ^0_m and E^0_m denote the zeroth-order Bloch functions and band-edge energies, respectively. In (A4) we have assumed the normalization $\langle\psi^0_m|\psi^0_m\rangle=1$ (which is used throughout this paper). Since H_{KP} is even with respect to the center of the Wigner-Seitz cell, only Bloch functions ψ^0_k with the same parity as ψ^0_m give a contri-

bution to ψ_m. Since the Bloch function at the band edge adjacent to m has different parity than ψ_m, this band edge does not contribute in the sum in (A4). Thus $\psi_m(x)$ can be written

$$\psi_m(x) = \psi_m^0(x) + V \sum_{k \neq m} c_{mk} \psi_k^0(x) + O(V^2) \ . \tag{A5}$$

It is easy to show that one can generally replace the periodic part of the band-edge Bloch function with the total band-edge Bloch function ψ in the expression for the interband matrix element p_{nm} in (11). To make the presentation valid for band edges with minima both at the zone center and at the zone edge, we will use the total wave function ψ below. We then have

$$p_{mn} = \frac{\int_c \psi_m^*(x)(-i\hbar \frac{d}{dx})\psi_n(x)dx}{\int_c \psi_m^*(x)\psi_m(x)dx} = \frac{\langle \psi_m | -i\hbar \frac{d}{dx} | \psi_n \rangle}{\langle \psi_m | \psi_m \rangle} \ . \tag{A6}$$

From (A5) one finds $\langle \psi_m | \psi_m \rangle = \langle \psi_m^0 | \psi_m^0 \rangle + O(V^2)$, and it is therefore consistent to replace $\langle \psi_m | \psi_m \rangle$ with $\langle \psi_m^0 | \psi_m^0 \rangle = 1$ in the denominator of (A6). For the numerator one has

$$\begin{aligned} \left\langle \psi_m \middle| \frac{d}{dx} \middle| \psi_n \right\rangle &= \left\langle \psi_m^0 \middle| \frac{d}{dx} \middle| \psi_n^0 \right\rangle \\ &+ V \left(\sum_{k \neq n} c_{nk} \left\langle \psi_m^0 \middle| \frac{d}{dx} \middle| \psi_k^0 \right\rangle \right. \\ &\left. + \sum_{k \neq m} c_{mk} \left\langle \psi_k^0 \middle| \frac{d}{dx} \middle| \psi_n^0 \right\rangle \right) + O(V^2) \ . \end{aligned} \tag{A7}$$

The lowest-order term in (A7) is nonzero only when m and n are adjacent band edges. For adjacent band edges it also follows that the correction terms of order V are zero. For nonadjacent band edges p_{mn} is of order V. Since $(E_m^0 - E_n^0) \sim O(V^0)$ for these band edges, the contributions to a_n and b_n from nonadjacent band edges are of order V. Thus to order V^0 the only contribution to a_n and b_n from the sum over band edges comes from the adjacent band edge.

For the band-edge energies we need the expansion

$$E_n = E_n^0 + \langle \psi_n^0 | H_{\mathrm{KP}} | \psi_n^0 \rangle + \sum_{m \neq n} \frac{|\langle \psi_m^0 | H_{\mathrm{KP}} | \psi_n^0 \rangle|^2}{E_n^0 - E_m^0} + \cdots \ . \tag{A8}$$

First we focus on the class-I conduction-band edge at $q_1 = \pi/a$ which is located at $k = \pi/a$ and is labeled $1c$. The properly normalized Bloch function at this band edge is $\psi_{1c}^0(x) = \sqrt{\frac{2}{a}} \cos(\pi x/a)$. The adjacent valence-band edge is labeled $1v$, and the corresponding Bloch function is $\psi_{1v}^0(x) = \sqrt{\frac{2}{a}} \sin(\pi x/a)$. From (17) and the discussion above it follows that

$$a_{1c} = 1 + \frac{-i\hbar p_{1v1c}}{m_0(E_{1c} - E_{1v})} \frac{\psi_{1v}'(0)}{\psi_{1c}(0)} + O(V) \ . \tag{A9}$$

Since $\psi_{1c}^0(x)$ is identically zero at the position of the δ wells, $\langle \psi_k^0 | H_{\mathrm{KP}} | \psi_{1c}^0 \rangle$ is zero for all k. Therefore $\psi_{1c}(x) = \psi_{1c}^0(x)$ and $\psi_{1c}(0) = \psi_{1c}^0(0) = \sqrt{\frac{2}{a}}$. In order to find $\psi_{1v}'(0)$ to order V one needs the Bloch function at all other valence-band edges with maxima at $k = \pi/a$. These are given by $\psi_{jv}^0(x) = \sqrt{\frac{2}{a}} \sin(q_j x)$, $q_j = \frac{j\pi}{a}$, $j = 3, 5, 7, \ldots$. We have

$$\psi_{1v}'(0) \simeq (\psi_{1v}^0)'(0) + \sum_{j \neq 1} \frac{\langle \psi_{jv}^0 | H_{\mathrm{KP}} | \psi_{1v}^0 \rangle}{E_{1v}^0 - E_{jv}^0} (\psi_{jv}^0)'(0) \ , \tag{A10}$$

and by using $E_j^0 = \frac{\hbar^2}{2m_0 a^2} j^2 \pi^2$, $\langle \psi_{jv}^0 | H_{\mathrm{KP}} | \psi_{1j}^0 \rangle = \frac{2\hbar^2}{m_0 a^2} V (-1)^{\frac{j+1}{2}}$, and $(\psi_{jv}^0)'(0) = \sqrt{\frac{2}{a}} \frac{j\pi}{a}$ one obtains to order V

$$\begin{aligned} \psi_{1v}'(0) &= \sqrt{\frac{2}{a}} \frac{\pi}{a} \left(1 - \frac{4V}{\pi^2} \sum_{j=3,5,7,\ldots} (-1)^{\frac{j+1}{2}} \frac{j}{j^2 - 1} \right) \\ &= \sqrt{\frac{2}{a}} \frac{\pi}{a} \left(1 - \frac{V}{\pi^2} \right) \ . \end{aligned} \tag{A11}$$

Since $\langle \psi_k^0 | H_{\mathrm{KP}} | \psi_{1c}^0 \rangle = 0$ for all k, E_{1c} equals E_{1c}^0, and one finds to order V^2 for the energy difference in (A9),

$$\begin{aligned} E_{1c} - E_{1v} &= E_{1c}^0 - E_{1v} \\ &= -\langle \psi_{1v}^0 | H_{\mathrm{KP}} | \psi_{1v}^0 \rangle - \sum_{j \neq 1} \frac{|\langle \psi_{jv}^0 | H_{\mathrm{KP}} | \psi_{1v}^0 \rangle|^2}{E_{1v}^0 - E_{jv}^0} \\ &= \frac{\hbar^2}{2m_0 a^2} \left(4V + \frac{16V^2}{\pi^2} \sum_{j=3,5,7,\ldots} \frac{1}{j^2 - 1} \right) \\ &= \frac{2\hbar^2}{m_0 a^2} V \left(1 + \frac{V}{\pi^2} \right) \ . \end{aligned} \tag{A12}$$

Finally, with

$$\begin{aligned} p_{1v1c} &= \frac{\langle \psi_{1v} | -i\hbar \frac{d}{dx} | \psi_{1c} \rangle}{\langle \psi_{1v} | \psi_{1v} \rangle} \\ &= \left\langle \psi_{1v}^0 \middle| -i\hbar \frac{d}{dx} \middle| \psi_{1c}^0 \right\rangle + O(V^2) \\ &= i\hbar \frac{\pi}{a} + O(V^2) \ , \end{aligned} \tag{A13}$$

one finds

$$\begin{aligned} a_{1c} &= 1 + \frac{-i\hbar p_{1v1c}}{m_0(E_{1c} - E_{1v})} \frac{\psi_{1v}'(0)}{\psi_{1c}(0)} + O(V) \\ &= 1 + \frac{2\pi^2}{4V} \left(1 - \frac{V}{\pi^2} \right) \left(1 + \frac{V}{\pi^2} \right)^{-1} + O(V) \\ &= \frac{\pi^2}{2V} + O(V) = \frac{m_0}{2m_{1c}^*} + O(V) \ , \end{aligned} \tag{A14}$$

where we have used the expression for the effective mass in (A3). Thus, we have shown that for the conduction-band edge at $q_1 = \pi/a$ there is to order V^0 no correction term to (28).

Next we consider the class-II conduction-band edge at $q_2 = 2\pi/a$ which is located at $k = 0$. The properly normalized Bloch function at this band edge is

$\psi^0_{2c}(x)=\sqrt{\frac{2}{a}}\sin(2\pi x/a)$, while the Bloch function at the adjacent band edge $2v$ is $\psi^0_{2v}(x)=\sqrt{\frac{2}{a}}\cos(2\pi x/a)$. In analogy to (A9), we have from (20) and the discussion above that

$$b_{2c}=\frac{-i\hbar p_{2v2c}}{m_0(E_{2c}-E_{2v})}\frac{\psi_{2v}(0)}{\psi'_{2c}(0)}+O(V)\,. \tag{A15}$$

Since $\psi^0_{2c}(x)$ is zero at the position of the δ wells, $\langle\psi^0_k|H_{\rm KP}|\psi^0_{2c}\rangle$ is zero for all k, and we have $\psi'_{2c}(0)=\psi^0_{2c}{}'(0)=\frac{2\pi}{a}\sqrt{\frac{2}{a}}$. In order to find $\psi_{2v}(0)$ to order V one needs the Bloch function at all the other valence-band edges with maxima at $k=0$. These are given by $\psi^0_{jv}(x)=\sqrt{\frac{2}{a}}\cos(q_jx)$, $q_j=\frac{j\pi}{a}$, $j=4,6,8,\ldots$. In addition one needs the unperturbed Bloch function at the bottom of the lowest band. This Bloch function is simply a constant, i.e., $\psi^0_0(x)=\sqrt{\frac{1}{a}}$. Thus

$$\psi_{2v}(0)\simeq\psi^0_{2v}(0)+\sum_{k\neq 2v}\frac{\langle\psi^0_k|H_{\rm KP}|\psi^0_{2v}\rangle}{E^0_{2v}-E^0_k}\psi^0_k(0). \tag{A16}$$

For the matrix elements in (A16) one finds $\langle\psi^0_0|H_{\rm KP}|\psi^0_{2v}\rangle=\frac{\hbar^2}{m_0a^2}\sqrt{2}V$, and $\langle\psi^0_{jv}|H_{\rm KP}|\psi^0_{2v}\rangle=\frac{\hbar^2}{m_0a^2}2V(-1)^{\frac{j}{2}}$, and with $E^0_j=\frac{\hbar^2}{2m_0a^2}j^2\pi^2$ and $\psi^0_{jv}(0)=\sqrt{\frac{2}{a}}$, one finds to order V

$$\begin{aligned}\psi_{2v}(0)&=\sqrt{\frac{2}{a}}\left(1+\frac{V}{2\pi^2}-\frac{4V}{\pi^2}\sum_{j=4,6,8,\ldots}\frac{(-1)^{\frac{j}{2}}}{j^2-4}\right)\\&=\sqrt{\frac{2}{a}}\left(1+\frac{V}{2\pi^2}-\frac{V}{4\pi^2}\right)=\sqrt{\frac{2}{a}}\left(1+\frac{V}{4\pi^2}\right)\,.\end{aligned} \tag{A17}$$

Since $\langle\psi^0_k|H_{\rm KP}|\psi^0_{2c}\rangle=0$ for all k, E_{2c0} equals E^0_{2c0} and one finds to order V^2 for the energy difference in (A15),

$$\begin{aligned}E_{2c}-E_{2v}&=E^0_{2c}-E_{2v}\\&=-\langle\psi^0_{2v}|H_{\rm KP}|\psi^0_{2v}\rangle-\sum_{k\neq 2v}\frac{|\langle\psi^0_k|H_{\rm KP}|\psi^0_{2v}\rangle|^2}{E^0_{2v}-E^0_k}\\&=\frac{\hbar^2}{2m_0a^2}\left(4V-\frac{2V^2}{\pi^2}+\frac{16V^2}{\pi^2}\sum_{j=4,6,8,\ldots}\frac{1}{j^2-4}\right)\\&=\frac{2\hbar^2}{m_0a^2}V\left(1+\frac{V}{4\pi^2}\right).\end{aligned} \tag{A18}$$

Thus, with

$$\begin{aligned}p_{2v2c}&=\frac{\langle\psi_{2v}|-i\hbar\frac{d}{dx}|\psi_{2c}\rangle}{\langle\psi_{2v}|\psi_{2v}\rangle}\\&=\left\langle\psi^0_{2v}\left|-i\hbar\frac{d}{dx}\right|\psi^0_{2c}\right\rangle+O(V^2)\\&=-i\hbar\frac{2\pi}{a}+O(V^2)\,,\end{aligned} \tag{A19}$$

one finally finds

$$\begin{aligned}b_{2c}&=\frac{-i\hbar p_{2v2c}}{m_0(E_{2c}-E_{2v})}\frac{\psi'_{2v}(0)}{\psi_{2c}(0)}+O(V)\\&=-\frac{a^2}{2V}\left(1+\frac{V}{4\pi^2}\right)\left(1+\frac{V}{4\pi^2}\right)^{-1}+O(V)\\&=-\frac{1}{2}\frac{m_0}{m^*_{2c}}\frac{1}{q_2^2}+O(V)\,,\end{aligned} \tag{A20}$$

where we have taken m^*_{2c} from (A3). Thus, we conclude that for the conduction-band edge at $q_2=2\pi/a$ also there is no correction term of order V^0 to the lowest-order result (31).

[1] G.H. Wannier, Phys. Rev. **52**, 191 (1937); J.C. Slater, *ibid.* **76**, 1592 (1949); H.M. James, *ibid.* **76**, 1611 (1949); J.M. Luttinger and W. Kohn, *ibid.* **97**, 869 (1955).

[2] See, for example, the reviews in D.L. Smith and C. Mailhiot, Rev. Mod. Phys. **62**, 173 (1990); G. Bastard, J.A. Brum, and R. Ferreira, Solid State Phys. **44**, 229 (1991); M.G. Burt, J. Phys. Condens. Matter **4**, 6651 (1992).

[3] R.A. Morrow, Phys. Rev. B **35**, 8074 (1987).

[4] J.W. Conley, C.B. Duke, G.D. Mahan, and J.J. Tiemann, Phys. Rev. **150**, 466 (1966).

[5] D.J. BenDaniel and C.B. Duke, Phys. Rev. **152**, 683 (1966).

[6] S.R. White and L.J. Sham, Phys. Rev. Lett. **47**, 879 (1981).

[7] G. Bastard, Phys. Rev. B **24**, 5693 (1981).

[8] I. Galbraith and G. Duggan, Phys. Rev. B **38**, 10 057 (1988).

[9] G.T. Einevoll and P.C. Hemmer, J. Phys. C **21**, L1193 (1988).

[10] G.T. Einevoll, P.C. Hemmer, and J. Thomsen, Phys. Rev. B **42**, 3485 (1990).

[11] G.T. Einevoll, Phys. Rev. B **42**, 3497 (1990).

[12] K. Young, Phys. Rev. B **39**, 13 434 (1989).

[13] See M.G. Burt in Ref. 2.

[14] H.C. Liu, Appl. Phys. Lett **51**, 1019 (1987).

[15] S.M. Sze, *Physics of Semiconductor Devices*, 2nd ed. (Wiley, New York, 1981).

[16] M. Altarelli in *Interfaces, Quantum Wells and Superlattices*, Vol. 179 of *NATO Advanced Study Institute, Series B: Physics*, edited by R. Leavens and R. Taylor (Plenum, New York, 1988).

[17] G.T. Einevoll and L.J. Sham, Phys. Rev. B **46**, 7787 (1992).

[18] R. Eppenga, M.F.H. Schuurmans, and S. Colak, Phys. Rev. B **36**, 1554 (1987).

[19] See, for example, L.J. Sham and Y.T. Lu, J. Lumin. **44**, 207 (1989).

[20] T. Ando, S. Wakahara, and H. Akera, Phys. Rev. B **40**, 11 609 (1989); T. Ando and H. Akera, *ibid.* **40**, 11 619 (1989).

[21] G.T. Einevoll, Ph.D. thesis, Norwegian Institute of Technology, Trondheim, 1991.

[22] G.T. Einevoll and P.C. Hemmer, Semicond. Sci. Technol. **6**, 590 (1991).